COMPARISON OF DIFFERENT NUMERICAL TECHNIQUES FOR THE DEVELOPMENT OF A SIMULATOR OF SURFACTANT ASSISTED ENHANCED OIL RECOVERY PROCESS

Kamilu Folorunsho Oyedeko[1] & Alfred Akpoveta Susu[2]
[1]Department of Chemical & Polymer Engineering, Lagos State University, Epe, Lagos, Nigeria
[2]Department of Chemical Engineering, University of Lagos, Lagos, Nigeria
E-mail:kfkoyedeko@yahoo.com; alfredasusu222@hotmail.com

ABSTRACT

In this work, a simulator is designed for enhanced oil recovery process for surfactant assisted water flooding. The system being investigated consists of three components (petroleum, water and surfactant) and two-phases (aqueous and oleic). The model equations are characterized by a system of non-linear, partial, differential equations: the continuity equation for the transport of each component, Darcy's equation for the flow of each phase and algebraic equations. The simulator incorporates first order effects, with scope to accommodate two or three dimensions, two fluid phases and one adsorbent phase and four other components. The numerical methods used in the solution of the model equations are the orthogonal collocation, finite difference, and coherence theory techniques. Matlab computer programs were used for the numerical solution of the model equations. The results of the orthogonal collocation solution were compared with those of finite difference and coherence solutions. The results indicate that the concentration of surfactants for orthogonal collocation show more features than the predictions of the coherence solutions and the finite difference, offering more opportunities for further understanding of the physical nature of the complex problem. Also, comparison of the orthogonal collocation solution with computations based on finite difference and coherence theory methods offers possible explanation for the observed differences especially between the methods and the two different reservoirs they represent.

Keywords: *Simulator Design; Multidimensional, Multiphase and Multicomponent system; Surfactant Flooding; Finite Difference Method; Orthogonal Collocation Technique; Coherence Theory Method.*

1. INTRODUCTION

The depleting world oil reserve can be conservatively managed through the use of tertiary production techniques known as Enhanced Oil Recovery procedures. Although production capacity can be enhanced through the primary and secondary recovery methods, bringing new fields online is very expensive and recovery from existing fields by conventional methods will not fully provide the necessary relief for global oil demand.

On an average, only about a third of the original oil in place can be recovered by the primary and secondary methods. The rest of the oil is trapped in reservoir pores due to surface and interfacial forces. This trapped oil can be recovered by reducing the capillary forces that prevent the oil from flowing within the pores of reservoir rock and into the well bores. Due to high oil prices and declining production in many regions around the globe, the possible application of advance technologies for further oil recovery, called "Enhanced Oil Recovery"(EOR) has become more attractive. The technology of EOR involves the injection of a fluid or fluids or materials into a reservoir to supplement the natural energy present in a reservoir, where the injected fluids interact with the reservoir rock/oil/brine system to create favourable conditions for maximum oil recovery. Surfactants are injected for this purpose to decrease the interfacial tension between oil and water in order to mobilize the oil trapped after secondary recovery by water flooding.

In a surfactant flood, a multi-component multiphase system is involved. The theory of multi-component, multiphase flow has been presented by several authors. The surfactant flooding is a form of chemical flooding process and is represented by a system of nonlinear, partial differential equations: the continuity equation for the transport of the components and Darcy's equation for the phase flow.

Systems of coupled, first-order, nonlinear hyperbolic partial differential equations (p.d.e.s) govern the transient evolution of a chemical flooding process for enhanced recovery. The method of characteristics (MOC) provides a way in which such systems of hyperbolic p.d.e.s can be solved by converting them to an equivalent system of ordinary differential equations. In fact, the MOC provides a similar framework for algorithm development to the coherence approach adopted here. In some cases, the characteristic solution has been used to track the flood-front in two-dimensional reservoir problems[1]. While the approach proposed by Ewing *et al.*[2], combines the characteristic method with a finite element approach. Zheng [3] has used the MOC and an adjustable number of moving particles to track three-dimensional solute fronts in groundwater systems; adjusting the number of particles serves to maintain an accurate material balance and save computational time. This front-tracking approach has been used in the present work to trace the movement of coherent waves, of both the diffuse and shock variety.

The concept of coherence was extended to general EOR processes[4,5], including alkaline flooding[6], convectional surfactant flooding[7], the effects of cation-exchange on surfactant-polymer flooding[8]. Refinements to the theory also allowed for equilibrium reaction to occur, such as precipitation-dissolution[9,10] and micelle formation[11]. Helset and Lake[12] have used simple wave theory (essentially identical to coherence theory) to study the one dimensional, three phase secondary migration of hydrocarbons from a source rock into possible reservoirs. Most recently, the theory of coherence has been applied successfully to the analysis of the transport of volatile compounds in porous media in the presence of a trapped gas phase[13].

At the simple level, the results of simulation using the principle of coherence are analogous to the Buckley-Leverett theory for waterflooding, the latter being evident in the work of Patton *et al.*[14] for polymer flooding, Fayers and Perrine[15] for dilute surfactant flooding, Claridge and Bondor[16] for carbonated water flooding, and Larson[17] and Hirasaki[7] for miscible and immiscible surfactant flooding, respectively, Pope, *et al.*[18] for isothermal, multiphase, multicomponent fluid flow in permeable media and Hankins and Harwell[19] for case studies in the feasibility of sweep improvement in surfactant-assisted water flooding.

High oil prices and declining production in many regions around the globe make enhanced oil recovery (EOR) increasingly attractive for investigators. As evident in the work of Siggel.et al[20] for a new class of viscoelastic surfactants for EOR, Xu and Lu [21] for microbially enhanced oil recovery at simulated reservoir conditions by use of engineered bacteria, Leach and Mason[22] for co-optimization of enhanced oil recovery and carbon sequestration, Harwell[23] for development of improved surfactants and EOR methods for small operators and many others.

The present work describes the development of a simulator for an Enhanced Oil Recovery process for surfactant assisted water flooding by applying different mathematical methods for solution of the model transport equations. The approach adopted here involves the use of different mathematical techniques, namely, orthogonal collocation method, finite difference and coherence theory methods for the development and solution of the relevant nonlinear partial differential equations. The different mathematical techniques are to be utilized to identify a particular type of physical behaviour and enable the understanding of the involved propagation phenomena. In particular, the techniques will be utilized for the prediction of what happens in EOR processes and possibly indicate how the reduction of the complexity of the problem.

The approach is multidimensional in that it involved at least three independent variables and the introduction of the concept of partial coherence which mean that the various composition path spaces required to map the composition routes of the system are at most two dimensional, allowing for a great simplification in complexity.

2. METHODOLOGY
This work considered solving multidimensional, multicomponent, multiphase flow problem associated with enhanced oil recovery process in petroleum engineering. The process of interest involves the injection of surfactant of different concentrations and pore volume to displace oil from the reservoir.
The methodology illustrates the steps utilized in executing the project using the developed mathematical models to describe the physics of reservoir depletion and fluid flow in which the areal distribution of fluids in the reservoir

resulting from a flood is one of its main aims. The system is for two or three dimensions, two fluid phases (aqueous, oleic) and one adsorbent phase, four components (oil, water, surfactants 1 and 2).

The reservoir may be divided into discrete grid blocks which may each be characterized by having different reservoir properties. The flow of fluids from a block is governed by the principle of mass conservation coupled with Darcy's law. The simultaneous flow of oil, gas, and water, in three dimensions and the effects of natural water influx, fluid compressibility, mass transfer between gas and liquid phases and the variation of such parameters as porosity and permeability, as functions of pressure are then modelled.

The model is developed from the basic law of conservation of mass[24]. The developed partial differential equation is converted to ordinary differential equation using coherent, finite difference and orthogonal collocation methods.

The finite difference method is a technique that converts partial differential equations into a system of linear equations. There are essentially three finite difference techniques. The explicit finite difference method converts the partial differential equations into an algebraic equation which can be solved by stepping forward (forward difference), backward (backward difference) or centrally (central difference).

The orthogonal collocation method converts partial differential equations into a system of ordinary differential equations using the lagrangian polynomial method. This set of ordinary differential equations generated is then solved with appropriate numerical technique such as Runge Kutta.

The coherent theory method combines the forward finite difference method with Runge Kutta technique to solve partial differential equations.

In the various solutions, several parameters are needed. The rock and fluid properties such as density, porosity, viscosity, oil and water etc, and other parameters are provided in Tables 1, 2, 3 and 4. Table 1 is the Reservoir characteristics from the work of Hankins and Harwell[24]. Table 2 is the Reservoir Characteristics used for the simulation work by Oyedeko[25]. Parameter values used in Trogus adsorption model for verification runs is shown in Table 3 while Table 4 presents additional reservoir parameters for the coherence work by Hankins and Harwell.[24]

In the present instance, in considering the more general form of the multiphase-multicomponent problem, the explicit Runge-Kutta method is chosen to solve the problem. The motivation for this explicit method is its simplicity and computational efficiency with the possibility of reducing truncation errors over those required for other methods.

The model encompasses two fluid phases (aqueous and oleic), one adsorbent phase (rock), and four components (oil, water, surfactants 1 and 2). The oil is displaced by water flooding. In-situ interaction of surfactant slugs may occur, with consequent phase separation and local permeability reduction. The model accommodates two (or three) physical dimensions, and an arbitrary, nonisotropic description of absolute permeability variation and porosity.

For most of the simulated cases in the work of Harkins and Harwell[24], the reservoir consisted of a rectangular composite of horizontal oil bearing strata, sandwiched above and below by two impervious rocks. Oil is produced from the reservoir by means of water injection at one end and a production well at the other. Data for the hypothetical reservoir simulated in Hankins and Harwell[24] are given in Table1 and the governing model equation is as shown by:

$$\phi S_w \frac{\partial C_{i,w}}{\partial t} + \rho(1-\phi)\frac{\partial \bar{C}_i}{\partial t} + \phi v_x f_w \frac{\partial C_{i,w}}{\partial x} + \phi v_y f_w \frac{\partial C_{i,w}}{\partial y} = -r_i \ (i=1,2) \qquad (1)$$

The term r_i represents the rate of loss of surfactant due to precipitation: for a one-to-one reaction stoichiometry, $r_1 = r_2$. Since reaction occurs instantaneously at a sharp interface, this term may be ignored away from the singular region of the interface.

It is possible to approximate the adsorption isotherm of a pure surfactant on a mineral oxide by use of a simple model. At low concentration, the adsorption obeys Henry's law, while above the critical micelle concentration (CMC) the total adsorption remains constant. The Trogus adsorption model[11,26] is used in this work.

2.1 Application of Coherence Theory to Solution of Model Equations

The material balance equations, Eqn. 1 (in the absence of r_i), are first order, homogeneous, nonlinear hyperbolic equations. Their solution will be attempted by means of the theory of coherence. The results presented here are general, and not restricted to assumptions regarding equilibrium relationships, fractional flow relationships, etc.

The concept of Coherence identifies the state which a dynamic, multi-component system strives to attain. The state of "coherence" requires all dependent variables at any given point in space and time to have the same wave velocity, giving rise to "a coherent" wave with no relative shift in the profiles of the variables. It has been established mathematically by Helfferich[27] that an arbitrary starting variation of dependent variables, if embedded between sufficiently large regions of constant state, is resolved into coherent waves, which become separated by new regions of constant state.

2.2.1 Oleic Partitioning

The model developed and expressed in Eqn.1 may be generalized by allowing

surfactants to partition into the oleic phase. In general, $C_{i,o} = C_{i,o}\left(C_{1,w}, C_{2,w}\right)$ this leads to:

$$\phi S_w \frac{\partial C_{i,w}}{\partial t} + \phi S_o \frac{\partial C_{i,o}}{\partial t} + \left(1-\phi\right)\rho \frac{\partial \bar{C}_{i,w}}{\partial t} + \phi v_x f_w \frac{\partial C_{i,w}}{\partial x} + \phi v_y f_w \frac{\partial C_{i,w}}{\partial y} + \phi v_x f_o \frac{\partial C_{i,o}}{\partial x} + \phi v_y f_o \frac{\partial C_{i,o}}{\partial x} = -r_i$$

(2)

Leading to the matrix equation:

$$\begin{bmatrix} \left(S_w + S_o p_{ii} + m_{11}\right)\lambda - f_w - f_o p_{11} & \left(S_o p_{12} + m_{12}\right)\lambda - f_o p_{12} \\ \left(S_o p_{21} + m_{21}\right)\lambda - f_o p_{21} & \left(S_w + S_o p_{22} + m_{22}\right)\lambda - f_w - f_o p_{22} \end{bmatrix} \times \begin{bmatrix} dC_{1,w} \\ dC_{2,w} \end{bmatrix} = 0$$

(3)

where

$$p_{i,j} = \frac{\partial C_{i,o}}{\partial C_{j,w}}, \quad f_o = 1 - f_w, \quad S_o = 1 - S_w$$

2.3 Application of Finite Difference to Solution of Model Equations

First-order, finite-difference expressions for the spatial derivatives were substituted into the hyperbolic chromatographic transport equations (Eq. 1), yielding 2 x m coupled ordinary differential equations which may then be integrated simultaneously (also known as the 'numerical method of lines').

$$s_w \frac{\partial C_{i,w}}{\partial \tau} + \sum_{j=1}^{2} m_{ij} \frac{\partial C_{i,w}}{\partial \tau} + f_w(\tau, \varepsilon_h) \times \left\{ \frac{C_{i,w}(\tau, \varepsilon_h) - C_{i,w}(\tau, \varepsilon_{h-1})}{\Delta \varepsilon} \right\} = 0$$

(4)

where $i = 1,2$ and $h = 1,2,. .. m$.

Eqn.4 is the finite-difference form of Eqn. 1 written for one spatial dimension ε, where m_{ij} are the adsorption coefficients, τ is dimensionless time (injected volume/ pore volume), and ε is dimensionless distance (pore volumes travelled). In two dimensions, the finite-difference terms are multiplied by dimensionless velocities. The distortion of the solution in the τ direction may be neglected by using a 4th order Runge-Kutta method and a sufficiently small time step.

The above equation is now transformed to the original form of Eqn. 1 using the already defined variables below:

$$C_{i,w}^{'} = \phi C_{i,w}$$

(5)

$$\bar{C}_{i}^{'} = \rho(1-\phi)\bar{C}_{i}^{'}$$

(6)

$$m_{i,j} = \frac{\partial \bar{C}_{i}^{'}}{\partial C_{j,w}^{'}}$$

(7)

Again, recall that differentiation of a function of another function (chain rule) is of the form:

$$\frac{\partial y}{\partial x} = \frac{\partial y}{\partial u} \times \frac{\partial u}{\partial x}$$

(8)

Applying the chain rule above, Eqn. 4 becomes:

$$S_w \frac{\partial C_{i,w}^{'}}{\partial \tau} + \left(\frac{\partial \bar{C}_{i}^{'}}{\partial C_{1,w}^{'}} \cdot \frac{\partial C_{1,w}^{'}}{\partial \tau} \right) + \left(\frac{\partial \bar{C}_{i}^{'}}{\partial C_{2,w}^{'}} \cdot \frac{\partial C_{2,w}^{'}}{\partial \tau} \right) + f_w(\tau, \varepsilon_h) \times \left\{ \frac{C_{i,w}^{'}(\tau, \varepsilon_h) - C_{i,w}^{'}(\tau, \varepsilon_{h-1})}{\Delta \varepsilon} \right\} = 0$$

(9)

Eliminating the primes (') and bars (-) and introducing $m_{i,j}$ terms yield:

$$(S_w + m_{11}) \frac{\partial C_{1,w}}{\partial \tau} + m_{12} \frac{\partial C_{2,w}}{\partial \tau} + f_w \frac{\partial C_{1,w}}{\partial \varepsilon} = 0$$

(10)

$$\left(S_w + m_{22}\right)\frac{\partial C_{2,w}}{\partial \tau} + m_{21}\frac{\partial C_{1,w}}{\partial \tau} + f_w\frac{\partial C_{2,w}}{\partial \varepsilon} = 0 \tag{11}$$

Applying the method of lines, a partial transformation to a difference equation, to the equations above yield:

$$\left(S_w + m_{11}\right)\frac{\partial C_{1,w}}{\partial \tau} + m_{12}\frac{\partial C_{2,w}}{\partial \tau} + f_w\frac{C_{1,w_{(\tau,\varepsilon_h)}} - C_{1,w_{(\tau,\varepsilon_h-1)}}}{\Delta\varepsilon} = 0 \tag{12}$$

$$\left(S_w + m_{22}\right)\frac{\partial C_{2,w}}{\partial \tau} + m_{21}\frac{\partial C_{1,w}}{\partial \tau} + f_w\frac{C_{2,w_{(\tau,\varepsilon_h)}} - C_{2,w_{(\tau,\varepsilon_h-1)}}}{\Delta\varepsilon} = 0 \tag{13}$$

This can also be written as follows:

$$\left(S_w + m_{11}\right)\frac{\partial C_{1,w_{(\tau,\varepsilon_h)}}}{\partial \tau} + m_{12}\frac{\partial C_{2,w_{(\tau,\varepsilon_h)}}}{\partial \tau} + \frac{f_w}{\Delta\varepsilon}\left[C_{1,w_{(\tau,\varepsilon_h)}} - C_{1,w_{(\tau,\varepsilon_h-1)}}\right] = 0 \tag{14}$$

$$\left(S_w + m_{22}\right)\frac{\partial C_{2,w_{(\tau,\varepsilon_h)}}}{\partial \tau} + m_{21}\frac{\partial C_{1,w_{(\tau,\varepsilon_h)}}}{\partial \tau} + \frac{f_w}{\Delta\varepsilon}\left[C_{2,w_{(\tau,\varepsilon_h)}} - C_{2,w_{(\tau,\varepsilon_h-1)}}\right] = 0 \tag{15}$$

Since we have a set of simultaneous ODE's, we will attempt to solve the equations:

$$\left(S_w + m_{11}\right)\frac{\partial C_{1,w_{(\tau,\varepsilon_h)}}}{\partial \tau} + m_{12}\frac{\partial C_{2,w_{(\tau,\varepsilon_h)}}}{\partial \tau} + \frac{f_w}{\Delta\varepsilon}\left[C_{1,w_{(\tau,\varepsilon_h)}} - C_{1,w_{(\tau,\varepsilon_h-1)}}\right] = 0 \tag{16}$$

$$\left(S_w + m_{22}\right)\frac{\partial C_{2,w_{(\tau,\varepsilon_h)}}}{\partial \tau} + m_{21}\frac{\partial C_{1,w_{(\tau,\varepsilon_h)}}}{\partial \tau} + \frac{f_w}{\Delta\varepsilon}\left[C_{2,w_{(\tau,\varepsilon_h)}} - C_{2,w_{(\tau,\varepsilon_h-1)}}\right] = 0 \tag{17}$$

where

$$m_{11} = \frac{\partial \overline{C}_1}{\partial C_{1,w}}$$

$$m_{12} = \frac{\partial \overline{C}_1}{\partial C_{2,w}}$$

$$m_{21} = \frac{\partial \overline{C}_2}{\partial C_{1,w}}$$

$$m_{22} = \frac{\partial \overline{C}_2}{\partial C_{2,w}}$$ Substituting for these terms in Eqs. 16 and 17 yield:

$$\left(S_w + \frac{\partial \overline{C}_1}{\partial C_{1,w}}\right)\frac{\partial C_{1,w_{(\tau,\varepsilon_h)}}}{\partial \tau} + \frac{\partial \overline{C}_1}{\partial C_{2,w}}\frac{\partial C_{2,w_{(\tau,\varepsilon_h)}}}{\partial \tau} + \frac{f_w}{\Delta\varepsilon}\left[C_{1,w_{(\tau,\varepsilon_h)}} - C_{1,w_{(\tau,\varepsilon_h-1)}}\right] = 0 \tag{18}$$

and

$$\left(S_w + \frac{\partial \overline{C}_2}{\partial C_{2,w}}\right)\frac{\partial C_{2,w_{(\tau,\varepsilon_h)}}}{\partial \tau} + \frac{\partial \overline{C}_2}{\partial C_{1,w}}\frac{\partial C_{1,w_{(\tau,\varepsilon_h)}}}{\partial \tau} + \frac{f_w}{\Delta \varepsilon}\left[C_{2,w_{(\tau,\varepsilon_h)}} - C_{2,w_{(\tau,\varepsilon_h-1)}}\right] = 0$$

(19)

These on simplification yield:

$$S_w \frac{\partial C_{1,w_{(\tau,\varepsilon_h)}}}{\partial \tau} + \frac{\partial \overline{C}_1}{\partial C_{1,w}} \cdot \frac{\partial C_{1,w_{(\tau,\varepsilon_h)}}}{\partial \tau} + \frac{\partial \overline{C}_1}{\partial C_{2,w}} \cdot \frac{\partial C_{2,w_{(\tau,\varepsilon_h)}}}{\partial \tau} + \frac{f_w}{\Delta \varepsilon}\left[C_{1,w_{(\tau,\varepsilon_h)}} - C_{1,w_{(\tau,\varepsilon_h-1)}}\right] = 0$$

$$S_w \frac{\partial C_{1,w_{(\tau,\varepsilon_h)}}}{\partial \tau} + \frac{\partial \overline{C}_1}{\partial \tau} + \frac{\partial \overline{C}_1}{\partial \tau} + \frac{f_w}{\Delta \varepsilon}\left[C_{1,w_{(\tau,\varepsilon_h)}} - C_{1,w_{(\tau,\varepsilon_h-1)}}\right] = 0$$

$$S_w \frac{\partial C_{1,w_{(\tau,\varepsilon_h)}}}{\partial \tau} + 2\frac{\partial \overline{C}_1}{\partial \tau} + \frac{f_w}{\Delta \varepsilon}\left[C_{1,w_{(\tau,\varepsilon_h)}} - C_{1,w_{(\tau,\varepsilon_h-1)}}\right] = 0$$

(20)

similarly

$$S_w \frac{\partial C_{2,w_{(\tau,\varepsilon_h)}}}{\partial \tau} + 2\frac{\partial \overline{C}_2}{\partial \tau} + \frac{f_w}{\Delta \varepsilon}\left[C_{2,w_{(\tau,\varepsilon_h)}} - C_{2,w_{(\tau,\varepsilon_h-1)}}\right] = 0$$

(21)

From the Trogus model[26],

$$\overline{C}_1 = k_1 C_{1,w}$$
$$\overline{C}_2 = k_2 C_{2,w}$$

A final substitution results in the equations below.

$$S_w \frac{\partial C_{1,w_{(\tau,\varepsilon_h)}}}{\partial \tau} + 2\frac{\partial (k_1 C_{1,w})}{\partial \tau} + \frac{f_w}{\Delta \varepsilon}\left[C_{1,w_{(\tau,\varepsilon_h)}} - C_{1,w_{(\tau,\varepsilon_h-1)}}\right] = 0$$

$$S_w \frac{\partial C_{1,w_{(\tau,\varepsilon_h)}}}{\partial \tau} + 2k_1 \frac{\partial C_{1,w}}{\partial \tau} + \frac{f_w}{\Delta \varepsilon}\left[C_{1,w_{(\tau,\varepsilon_h)}} - C_{1,w_{(\tau,\varepsilon_h-1)}}\right] = 0$$

$$(S_w + 2k_1)\frac{\partial C_{1,w}}{\partial \tau} + \frac{f_w}{\Delta \varepsilon}\left[C_{1,w_{(\tau,\varepsilon_h)}} - C_{1,w_{(\tau,\varepsilon_h-1)}}\right] = 0$$

(22)

and

$$S_w \frac{\partial C_{2,w_{(\tau,\varepsilon_h)}}}{\partial \tau} + 2\frac{\partial (k_2 C_{2,w})}{\partial \tau} + \frac{f_w}{\Delta \varepsilon}\left[C_{2,w_{(\tau,\varepsilon_h)}} - C_{2,w_{(\tau,\varepsilon_h-1)}}\right] = 0$$

$$(S_w + 2k_2)\frac{\partial C_{2,w}}{\partial \tau} + \frac{f_w}{\Delta \varepsilon}\left[C_{2,w_{(\tau,\varepsilon_h)}} - C_{2,w_{(\tau,\varepsilon_h-1)}}\right] = 0$$

(23)

2.4 Application of Orthogonal Collocation to Solution of Model Equations
Equation 1 can be written as:

$$S_w \frac{\partial C_{i,w}^{'}}{\partial \tau} + 2 \frac{\partial \bar{C_i^{'}}}{\partial \tau} + f_w(\tau, \varepsilon_h) \times \left\{ \frac{C_{i,w}^{'}(\tau, \varepsilon_h) - C_{i,w}^{'}(\tau, \varepsilon_{h-1})}{\Delta \varepsilon} \right\} = 0 \tag{24}$$

$$S_w \frac{\partial [\phi C_{i,w}]}{\partial \tau} + 2 \frac{\partial [\rho(1-\phi)\bar{C_i}]}{\partial \tau} + f_w(\tau, \varepsilon_h) \times \left\{ \frac{[\phi C_{i,w}](\tau, \varepsilon_h) - [\phi C_{i,w}](\tau, \varepsilon_{h-1})}{\Delta \varepsilon} \right\} = 0 \tag{25}$$

$$\phi S_w \frac{\partial C_{i,w}}{\partial \tau} + 2\rho(1-\phi) \frac{\partial \bar{C_i}}{\partial \tau} + \phi f_w(\tau, \varepsilon_h) \times \left\{ \frac{C_{i,w}(\tau, \varepsilon_h) - C_{i,w}(\tau, \varepsilon_{h-1})}{\Delta \varepsilon} \right\} = 0 \tag{26}$$

Now, from the Trogus model[26],

$$\bar{C_i} = \kappa_i C_{i,w} \tag{27}$$

$$\phi S_w \frac{\partial C_{i,w}}{\partial \tau} + 2\rho(1-\phi) \frac{\partial (\kappa_i C_{i,w})}{\partial \tau} + \phi f_w(\tau, \varepsilon_h) \times \left\{ \frac{C_{i,w}(\tau, \varepsilon_h) - C_{i,w}(\tau, \varepsilon_{h-1})}{\Delta \varepsilon} \right\} = 0 \tag{28}$$

$$\phi S_w \frac{\partial C_{i,w}}{\partial \tau} + 2\kappa_i \rho(1-\phi) \frac{\partial C_{i,w}}{\partial \tau} + \phi f_w(\tau, \varepsilon_h) \times \left\{ \frac{C_{i,w}(\tau, \varepsilon_h) - C_{i,w}(\tau, \varepsilon_{h-1})}{\Delta \varepsilon} \right\} = 0 \tag{29}$$

$$\phi S_w \frac{\partial C_{i,w}}{\partial \tau} + 2\kappa_i \rho(1-\phi) \frac{\partial C_{i,w}}{\partial \tau} + \phi f_w(\tau, \varepsilon_h) \frac{\partial C_{i,w}}{\partial \varepsilon} = 0 \tag{30}$$

$$[\phi S_w + 2\kappa_i \rho(1-\phi)] \frac{\partial C_{i,w}}{\partial \tau} + \phi f_w(\tau, \varepsilon_h) \frac{\partial C_{i,w}}{\partial \varepsilon} = 0 \tag{31}$$

Let

$$R = [\phi S_w + 2\kappa_i \rho(1-\phi)]$$
$$B = \phi f_w$$

The above equations now become:

$$R \frac{\partial C}{\partial \tau} + B \frac{\partial C}{\partial \varepsilon} = 0 \tag{32}$$

where C is a function of both ε (dimensionless distance) and τ (dimensionless time).

Using the method of orthogonal collocation, let C be approximated by the expression:

$$C(\tau,\varepsilon) = \sum_{I=1}^{N+1} C_I(\tau) X_J(\varepsilon_I) \tag{33}$$

Equation 32 can now be expressed as follows:

$$R\frac{\partial C}{\partial \tau} + B\frac{\partial}{\partial \varepsilon}\sum_{I=1}^{N+1} C_I(\tau) X_J(\varepsilon_I) = 0 \tag{34}$$

$$R\frac{\partial C}{\partial \tau} + B\sum_{I=1}^{N+1}\frac{\partial}{\partial \varepsilon}[C_I(\tau) X_J(\varepsilon_I)] = 0 \tag{35}$$

$$R\frac{\partial C}{\partial \tau} + B\sum_{I=1}^{N+1}\frac{\partial}{\partial \varepsilon}[X_J(\varepsilon_I)].C_I(\tau) = 0 \tag{36}$$

$$a_{JI} = \frac{\partial}{\partial \varepsilon} X_J(\varepsilon_I) \tag{37}$$

$$R\frac{\partial C_J}{\partial \tau} + B\sum_{I=1}^{N+1} a_{JI}C_I = 0 \tag{38}$$

$$\frac{\partial C_J}{\partial \tau} + \frac{B}{R}\sum_{I=1}^{N+1} a_{JI}C_I = 0 \tag{39}$$

$$\frac{\partial C_J}{\partial \tau} = -\frac{B}{R}\sum_{I=1}^{N+1} a_{JI}C_I \tag{40}$$

For I = 1, 2, 3, 4… N+1

Therefore,

$$\frac{\partial C_J}{\partial \tau} = -\frac{B}{R}\left[a_{J1}C_1 + a_{J2}C_2 + a_{J3}C_3 + a_{J4}C_4 +...+ a_{JN+1}C_{N+1}\right] \tag{41}$$

Again J = 1, 2, 3, 4… N+1

Therefore the following system of ODE's can be generated:

$$\frac{\partial C_1}{\partial \tau} = -\frac{B}{R}\left[a_{11}C_1 + a_{12}C_2 + a_{13}C_3 + a_{14}C_4 +...+ a_{1N+1}C_{N+1}\right]$$

$$\frac{\partial C_2}{\partial \tau} = -\frac{B}{R}\left[a_{21}C_1 + a_{22}C_2 + a_{23}C_3 + a_{24}C_4 +...+ a_{2N+1}C_{N+1}\right]$$

$$\frac{\partial C_3}{\partial \tau} = -\frac{B}{R}\left[a_{31}C_1 + a_{32}C_2 + a_{33}C_3 + a_{34}C_4 + ... + a_{3N+1}C_{N+1}\right]$$

$$\frac{\partial C_4}{\partial \tau} = -\frac{B}{R}\left[a_{41}C_1 + a_{42}C_2 + a_{43}C_3 + a_{44}C_4 + ... + a_{4N+1}C_{N+1}\right]$$

$$\vdots \frac{\partial C_{N+1}}{\partial \tau} = -\frac{B}{R}\left[a_{N+11}C_1 + a_{N+12}C_2 + a_{N+13}C_3 + a_{N+14}C_4 + ... + a_{N+1N+1}C_{N+1}\right]$$

(42)

In matrix form, we have the following expression:

$$
\begin{bmatrix}
\dfrac{\partial C_1}{\partial \tau} \\[2mm]
\dfrac{\partial C_2}{\partial \tau} \\[2mm]
\dfrac{\partial C_3}{\partial \tau} \\[2mm]
\dfrac{\partial C_4}{\partial \tau} \\[2mm]
\vdots \\
\vdots \\
\vdots \\
\vdots \\
\vdots \\
\vdots \\
\dfrac{\partial C_{N+1}}{\partial \tau}
\end{bmatrix}
= -\frac{B}{R}
\begin{bmatrix}
a_{11} & a_{12} & a_{13} & a_{14} & ... & ... & ... & ... & ... & a_{1N+1} \\
a_{21} & a_{22} & a_{23} & a_{24} & & & & & & a_{2N+1} \\
a_{31} & \vdots & & & & & & & & a_{3N+1} \\
a_{41} & \vdots & & & & & & & & a_{4N+1} \\
\vdots & \vdots & & & & & & & & \\
\vdots & \vdots & & & & & & & & \\
\vdots & \vdots & & & & & & & & \\
\vdots & \vdots & & & & & & & & \\
\vdots & \vdots & & & & & & & & \\
a_{N+11} & a_{N+12} & ... & ... & ... & ... & ... & ... & ... & a_{N+1N+1}
\end{bmatrix}
\begin{bmatrix}
C_1(\tau) \\
C_2(\tau) \\
C_3(\tau) \\
C_4(\tau) \\
\vdots \\
\vdots \\
\vdots \\
\vdots \\
\vdots \\
C_{N+1}(\tau)
\end{bmatrix}
$$

(43)

Similarly, the following expression defines a_{JI} [28,29] :

$$
a_{JI} = \begin{cases}
\dfrac{1}{2}\dfrac{P_{N+1}^{(2)}(\varepsilon_I)}{P_{N+1}^{(1)}(\varepsilon_I)} & \text{For J = I} \\[4mm]
\dfrac{1}{\varepsilon_I - \varepsilon_J}\dfrac{P_{N+1}^{(1)}(\varepsilon_I)}{P_{N+1}^{(1)}(\varepsilon_J)} & \text{For I} \neq \text{J}
\end{cases}
$$

(44)

where

$$P_J(\varepsilon) = (\varepsilon - \varepsilon_J)P_{J-1}(\varepsilon); J = 1,2,3,...,N+1$$

$$P_J^{(1)}(\varepsilon) = (\varepsilon - \varepsilon_J)P_{J-1}^{(1)}(\varepsilon) + P_{J-1}(\varepsilon)$$

$$P_J^{(2)}(\varepsilon) = (\varepsilon - \varepsilon_J)P_{J-1}^{(2)}(\varepsilon) + 2P_{J-1}^{(1)}(\varepsilon)$$

$$P_0^{(1)}(\varepsilon) = P_0^{(2)}(\varepsilon) = 0$$

$$P_0(\varepsilon) = 1 \tag{45}$$

Recall that the elements of the matrix can be generated from the following Lagrange polynomial.

$$a_{ij} = \frac{dl_j(x_i)}{dx} = \begin{cases} \dfrac{1}{2}\dfrac{P_{N+1}^{(2)}(x_i)}{P_{N+1}^{(1)}(x_i)} & j=i \\[3mm] \dfrac{1}{x_i - x_j}\dfrac{P_{N+1}^{(1)}(x_i)}{P_{N+1}^{(1)}(x_j)} & i \neq j \end{cases} \tag{46}$$

For i = j, the elements here refer to the leading diagonal of the matrix to be generated
For i ≠ j, the elements here refer to all other elements of the matrix
Also, the following recurrence relations are defined below.

$$p_o(x) = 1$$

$$P_j(x) = (x - x_j)P_{j-1}(x)$$

$$P_j^{(1)}(x) = (x - x_j)P_{j-1}^{(1)}(x) + P_{j-1}(x)$$

$$P_j^{(2)}(x) = (x - x_j)P_{j-1}^{(2)}(x) + 2P_{j-1}^{(1)}(x) \tag{47}$$

For j = 2, 3, 4, ..., N+1
The following substitutions and manipulations will now be made to redefine equation 46
Substituting the recurrence relations into Eqn. 46 yields:

$$a_{ij} = \begin{cases} \dfrac{1}{2}\left[\dfrac{(x_i - x_j)P_{j-1}^{(2)}(x_i) + 2P_{j-1}^{(1)}(x_i)}{(x_i - x_j)P_{j-1}^{(1)}(x_i) + P_{j-1}(x_i)}\right] & j=i \\[4mm] \dfrac{1}{x_i - x_j}\left[\dfrac{(x_i - x_j)P_{j-1}^{(1)}(x_i) + P_{j-1}(x_i)}{(x_j - x_j)P_{j-1}^{(1)}(x_j) + P_{j-1}(x_j)}\right] & i \neq j \end{cases} \tag{48}$$

Now, some terms will be cancelled out
Since j = i,
(x$_i$ – x$_j$) = 0
and
(x$_j$ – x$_j$)=0

$$a_{ij} = \begin{cases} \dfrac{1}{2}\left[\dfrac{2P_{j-1}^{(1)}(x_i)}{P_{j-1}(x_i)} \right] & j=i \\[4mm] \dfrac{1}{x_i - x_j}\left[\dfrac{(x_i - x_j)P_{j-1}^{(1)}(x_i) + P_{j-1}(x_i)}{P_{j-1}(x_j)} \right] & i \neq j \end{cases}$$

(49)

The above becomes:

$$a_{ij} = \begin{cases} \left[\dfrac{P_{j-1}^{(1)}(x_i)}{P_{j-1}(x_i)} \right] & j=i \\[4mm] \dfrac{(x_i - x_j)P_{j-1}^{(1)}(x_i)}{(x_i - x_j)P_{j-1}(x_j)} + \dfrac{1}{x_i - x_j}\left[\dfrac{P_{j-1}(x_i)}{P_{j-1}(x_j)} \right] & i \neq j \end{cases}$$

(50)

This becomes:

$$a_{ij} = \begin{cases} \left[\dfrac{P_{j-1}^{(1)}(x_i)}{P_{j-1}(x_i)} \right] & j=i \\[4mm] \dfrac{P_{j-1}^{(1)}(x_i)}{P_{j-1}(x_j)} + \dfrac{1}{x_i - x_j}\left[\dfrac{P_{j-1}(x_i)}{P_{j-1}(x_j)} \right] & i \neq j \end{cases}$$

(51)

Rewriting the above in terms of epsilon, (ε), we have:

$$a_{ij} = \begin{cases} \left[\dfrac{P_{j-1}^{(1)}(\varepsilon_i)}{P_{j-1}(\varepsilon_i)} \right] & j=i \\[4mm] \dfrac{P_{j-1}^{(1)}(\varepsilon_i)}{P_{j-1}(\varepsilon_j)} + \dfrac{1}{\varepsilon_i - \varepsilon_j}\left[\dfrac{P_{j-1}(\varepsilon_i)}{P_{j-1}(\varepsilon_j)} \right] & i \neq j \end{cases}$$

(52)

The matrix now looks like this:

$$a_{11} = \frac{P_0^{(1)}(\varepsilon_1)}{P_0(\varepsilon_1)}$$

$$a_{12} = \frac{P_1^{(1)}(\varepsilon_1)}{P_1(\varepsilon_2)} + \frac{1}{\varepsilon_1 - \varepsilon_2}\frac{P_1(\varepsilon_1)}{P_1(\varepsilon_2)}$$

$$a_{13} = \frac{P_2^{(1)}(\varepsilon_1)}{P_2(\varepsilon_3)} + \frac{1}{\varepsilon_1 - \varepsilon_2}\frac{P_2(\varepsilon_1)}{P_2(\varepsilon_3)}$$

$$a_{21} = \frac{P_0^{(1)}(\varepsilon_2)}{P_0(\varepsilon_1)} + \frac{1}{\varepsilon_2 - \varepsilon_1} \frac{P_0(\varepsilon_2)}{P_0(\varepsilon_1)}$$

$$a_{22} = \frac{P_1^{(1)}(\varepsilon_2)}{P_1(\varepsilon_1)}$$

$$a_{23} = \frac{P_2^{(1)}(\varepsilon_2)}{P_2(\varepsilon_3)} + \frac{1}{\varepsilon_2 - \varepsilon_3} \frac{P_2(\varepsilon_2)}{P_2(\varepsilon_3)}$$

$$a_{31} = \frac{P_0^{(1)}(\varepsilon_3)}{P_0(\varepsilon_1)} + \frac{1}{\varepsilon_3 - \varepsilon_1} \frac{P_0(\varepsilon_3)}{P_0(\varepsilon_1)}$$

$$a_{32} = \frac{P_1^{(1)}(\varepsilon_3)}{P_1(\varepsilon_2)} + \frac{1}{\varepsilon_3 - \varepsilon_2} \frac{P_1(\varepsilon_3)}{P_1(\varepsilon_2)}$$

$$a_{32} = \frac{P_2^{(1)}(\varepsilon_3)}{P_2(\varepsilon_3)} \tag{53}$$

The recurrence relations below will again be used to evaluate the terms of the matrix.

$$p_o(\varepsilon) = 1$$
$$P_j(\varepsilon) = (\varepsilon - \varepsilon_j)P_{j-1}(\varepsilon)$$
$$P_j^{(1)}(\varepsilon) = (\varepsilon - \varepsilon_j)P_{j-1}^{(1)}(\varepsilon) + P_{j-1}(\varepsilon)$$
$$P_0^{(1)}(\varepsilon) = 0 \tag{54}$$

Let ε assume the range

ε = [0:0.01:0.09]

where

$$\varepsilon_1 = 0 \tag{55}$$

$$\varepsilon_2 = 0.01 \tag{56}$$

$$\varepsilon_3 = 0.02 \tag{57}$$

3.   RESULTS
The reservoir response, as predicted by the simulation on the basis of the theory of coherence, is compared with the numerical predictions obtained using traditional finite difference method and orthogonal collocation. The case studies are chosen to be both hypothetical and using of existing Nigerian well data with simple representative of the important elements of the simulator. The main objective of these case studies has been to demonstrate that the mathematical techniques of orthogonal collocation, finite difference and coherent theory in the context of

application of the simulator can be used to obtain wave behaviour in a reservoir. A gradually increasing level of complexity is introduced, representing a range of systems from aqueous phase flow, to surfactant chromatography in two phase flow, to surfactant chromatography in two dimensional porous medium. The initial and injected surfactant compositions corresponding to cases 1, 2 and 3 are shown in Table 5. The rock and fluid properties are listed in Table 1, 2, 3, 4. These were taken as uniform for convenience.

The two fluid phases consisted of a water phase and an oil phase, which, for convenience are considered incompressible. The density of oil, the viscosity of oil, the salinity of water, and the formation volume factor of oil and water are listed in Table 2 in appendix. All cases mentioned above were run by using anionic sodium dodecyl sulfate (SDS) and cationic dodecyl pyridinium chloride (DPC) as surfactants.

The system of equations is complete with the equations representing physical properties of the fluids and the rock. The physical properties described here are: (1) phase behaviour (2) interfacial tension between fluid phases, (3) residual phase saturations, (4) relative permeabilities, (5) rock wettabiliy, (6) phase viscosities, (7) capillary pressure, (8) adsorption and (9) dispersion. From a physical-chemical point of view, there are three components - water, petroleum and chemical. They are in fact, pseudo-components, since each one consists of several pure components. Petroleum is a complex mixture of many hydrocarbons. Water is actually brine, and contains dissolved salts. Finally, the chemical contains different kinds of surfactants.

These three pseudo-components are distributed between two phases –the oleic phase and the aqueous phase. The chemical has an amphiphilic character. It makes the oleic phase at least partially miscible with water or the aqueous phase at partially miscible with petroleum. Interfacial tension depends on the surfactant partition between the two phases, and hence of phase behaviour. Residual phase saturation decreases as interfacial tension decreases. Relative permeability parameters depend on residual phase saturations. Phase viscosities are functions of the volume fraction of the components in each fluid phase. Therefore, the success or failure of surfactant flooding processes depends on phase behaviour. Phase behaviour influences all other physical properties, and each of them, in turn influences oil recovery.

For a two-phase flow of water and oil, where no surfactant partitions into the oleic phase, the same scenario is obtained as the one dimensional injection for cases 1 and 2. The bed has an initial water saturation of 0.3, and is flooded with an aqueous surfactant solution. The numerical profiles agree with the coherent wave profiles. The effect of the two–phase flow is to elongate the waves, leading to a larger region of constant state and earlier breakthrough of the fast wave.

Figure 1a is the result obtained for solving Equation 4 using the three methods finite difference, orthogonal collocation, coherent theory. The graph is for the composition profile for one dimensional two-phase chromatography initially equilibrated with a composition C1 = 0.21, C2 = 0.181 and is then injected with a composition C1 = 0.17, C2 = 0.013 (Riemann type problem, Case 1 (refer to Table 5)). In Figure 1a, the profile C1 of finite difference shows a steady rise from C1 = 0.17 to C1= 0.21 and then remain constant at this concentration. The profile C1 of the orthogonal collocation increases steadily from C1 = 0.17 to C1 = 0.21 at distance 0.1 epsilon maintaining a constant state to distance 0.3 epsilon. After this it started declining from C1 = 0.21 to C1 = 0.07 at distance 0.5 epsilon before rising back to attain a constant state with the finite difference. The profile C1 of the coherent theory on the other hand started with a constant state, then declined before continues with constant state and rise again to attain constant state with the other profiles. Similarly, the profile C2 of finite difference increased steadily from C2 = 0.017 to a constant state of C2 = 0.18 The orthogonal collocation for C_2 starts at C2 = 0.01 for a short constant state and then rise steadily to C2 = 0.18 to attain another short constant state from 0.2 to 0.3 epsilon. From here it depressed to C2 = 0.07 before rising back to C2 = 0.18 and then attain a constant state with finite difference. The profile C2 of coherent theory starts with a short constant state, then increases readily to C2 = 0.05 for another constant state from which it rises up to the final region of constant state with the other profiles.

Figure 1b shows the result obtained for solving Eqn. 4 by using orthogonal collocation and finite difference as the numerical technique. The graph is for the bed composition profile for one dimensional two-phase phase chromatography for case 1 at one pore volume injected. In this case also, the adsorbing porous medium is initially equibrated with a composition. C1 = 0.21, C2 = 0.181 (concentrations normalized as moles in solution per m^3 off bed) and is then injected with a composition C1 = 0.17, C2 = 0.013 (Riemann-type problem, Case 1 (refer to Table 5)). The profile C1 of finite difference indicates rise in concentration from C1 = 0.17 to 0.21 after which the concentratiopn maintained a constant state. The profile of C1 of the orthogonal collocation also rise from C1 = 0.17 to C1 = 0.21 but falls to 0.03 epsilon at distance 0.4 epsilon and then increased steadily to constant state as for C1 finite difference. The profile C1 of coherent theory indicates that it started with a constant concentration and decreased gradually to attain another region of constant state.The profile C2 of finite difference increased steadily from C2 = 0.02 to attain constant state at 0.18 epsilon. Also the profile of C2 of the orthogonal collocation increase gradually from C2 = 0.02 to C1 = 0.18 at distance 0.2 for a short constant state and then decline to a low value of C2 = 0.02 at distance 0.4 epsilon before rising back to reach a constant state with the finite difference. The profile C2 of coherent theory started with a constant state and gradually rise to a state of constant state .

The bed composition profile for one dimensional two-phase chromatography for case 1 at two pore volume injected is shown in Figure 1c. This is the result obtained for solving Equation 4 by using these three techniques; finite difference, orthogonal collocation and coherent theory. The adsorbing porous medium is initially equibrated with a composition. C1 = 0.21, C2 = 0.181 (concentrations normalized as moles in solution per m^3 off bed) and is then injected with a composition C1 = 0.17, C2 = 0.013 (Riemann-type problem: Case 1 (refer to Table 5)). The profile C_1 of finite difference and the profile C1 of orthogonal collocation indicate that there is steady increase from C1 = 0.17 to C1 = 0.21 at distance 0.1 epsilon and then attained a constant state for both profiles. However, the profile C_1 of coherent theory shows a constant state of concentration at C1 = 0.04 before having a self sharpening shock of C1 = 0.05, and eigenvalue λ = 0.499. It then continues with a constant state and decreased to zero at distance 0.73. Similarly, the profile C_2 of finite difference shows a steady rise from C2 = 0.02 to C2 = 0.18 and then maintained a constant state. Also, the profile C2 for orthogonal collocation, follows the same pattern, which indicates an increase from C2 = 0.02 to C2 = 0.18 and then attained a constant state. The orthogonal collocation profiles match the finite difference profiles. However, the profile C2 of coherent theory shows a constant state of concentration but has no self sharpening. C_2 = 0.00 in this case before its termination at distance 0.499 epsilon.
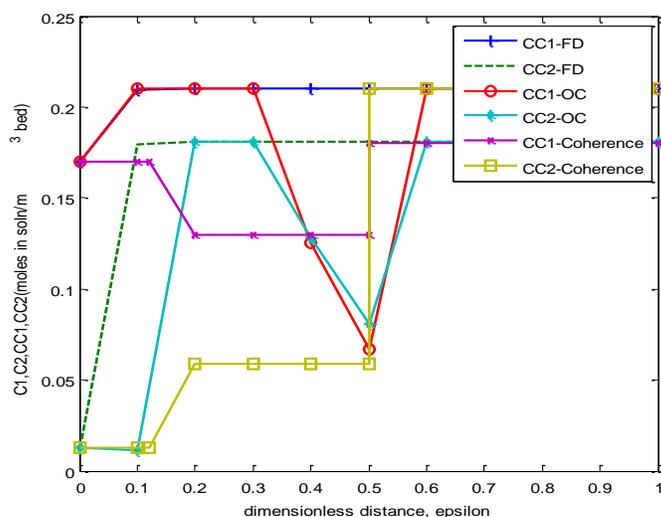

Figure 1a, Case 1. C1,C2,CC1,CC2 vs epsilon at τ = 0.5. Bed composition profile for one-dimensional two-phase chromatography; Case 1, at one-half pore volume injected. The plots are for three methods: Orthogonal collocation(OC), finite difference(FD) and coherent theory(CT)
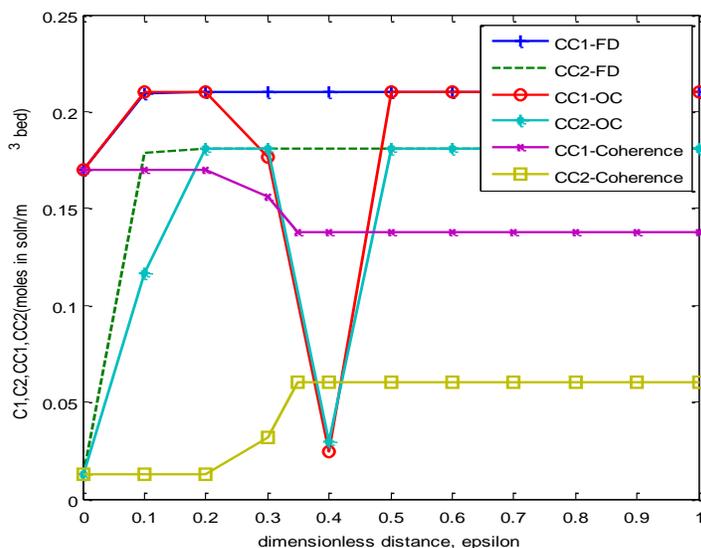
Figure 1b. Case 1. C1,C2,CC1,CC2 vs epsilon at τ = 1.0. Bed composition profile for one-dimensional two-phase chromatography; Case 1 at one pore volume injected. The plots are for three methods: Orthogonal collocation(OC), finite difference(FD) and coherent theory(CT)
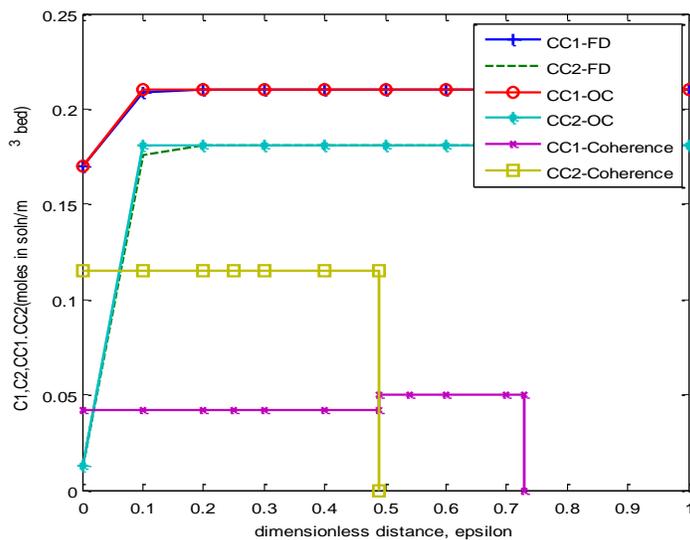

Figure 1c. Case 1. C1,C2,CC1,CC2 vs epsilon at τ = 2.0. Bed composition profile for one-dimensional two-phase chromatography; Case 1, at two pore volumes injected. The plots are for three methods: Orthogonal collocation(OC), finite difference(FD) and coherent theory(CT)

Figure 2a shows the bed concentration profiles for one dimensional two-phase chromatography for case 2 at one pore volume injected in the porous medium initially devoid of surfactant and then injected with a mixture C1 = 0.042, C2 = 0.115 (Riemann-type problem, Case 2 (refer to Table 5)), with the numerical result obtained for solving Eqn. 4 by using three different techniques: orthogonal collocation, finite difference and coherent theory. The profile C1 of finite difference shows steady decline from C1 = 0.04 to a constant state. Also, the C1 of orthogonal collocation falls steadily from C1= 0.04 to a constant state as for finite difference. However, the profile C_1 of

coherent theory shows a constant state of concentration at C1 = 0.04 before having a self sharpening shock of C1 = 0.048, and eigenvalue λ = 0.26. It then continues with a constant state and decreased to zero at distance 0.37. The profile C2 of finite difference decreased steadily from C2 = 0.119 to C2 = 0.001 and then to a constant state as for C1. Similarly, the C2 of orthogonal collocation falls steadily from C2 = 0.119 to C2 = 0.001 and gradually to a constant state as finite difference. However, the profile C2 of coherent theory shows a constant state of concentration but has no self sharpening. C1 = 0.00 in this case before its termination at distance 0.26 epsilon.

The bed composition profile for one dimensional two-phase chromatography for case 2 at two pore volume injected is shown in Figure 2b. This is the result obtained for solving Equation 4 by using these three techniques; finite difference, orthogonal collocation and coherent theory. In figure 5b, the profile C1 of finite difference shows steady decline from from C1 = 0.04 to a constant state. Also the C1 of orthogponal collocation falls steadily from C1 = 0.04 to a constant state as for finite difference. While the profile C1 of coherent theory shows a constant state of concentration at C1 = 0.04 before having a self sharpening shock of C1 = 0.046, and eigenvalue λ = 0.53. It then continues with a constant state and decreased to zero at distance 0.84 epsilon. The profile C2 of finite difference decreased steadily from C2 = 0.119 to C2 = 0.001 and then to a constant state as for C1. Similarly, the C2 of orthogonal collocation falls steadily from C2 = 0.119 to C2 = 0.001 and then to a constant state as finite difference.

In Figure 2b, the profiles C1 of orthogonal collocation, finite difference and coherent theory follow the same pattern as that in Figure 2a. Similarly, the profiles C2 of finite difference, orthogonal collocation, coherent theory in Figure 2a have the same pattern as those in Figure 2b.

Figure 2a. Case 2. C1,C2,CC1,CC2 vs epsilon at τ = 1.0. Bed composition profile for one-dimensional two-phase chromatography; Case 2, at one pore volume injected The plots are for three methods: Orthogonal collocation(OC), finite difference(FD) and coherent theory(CT).
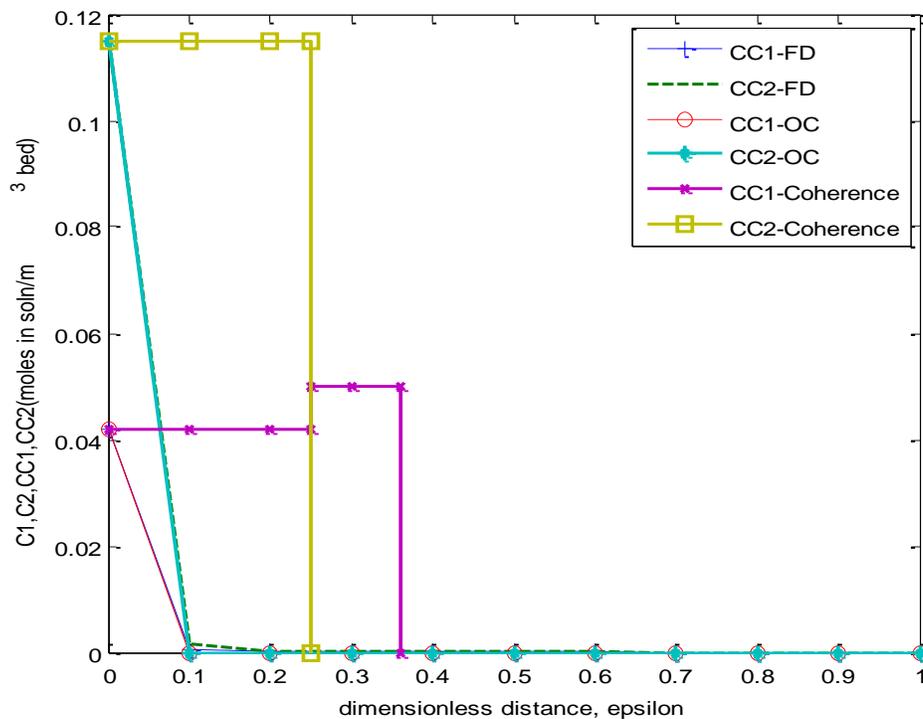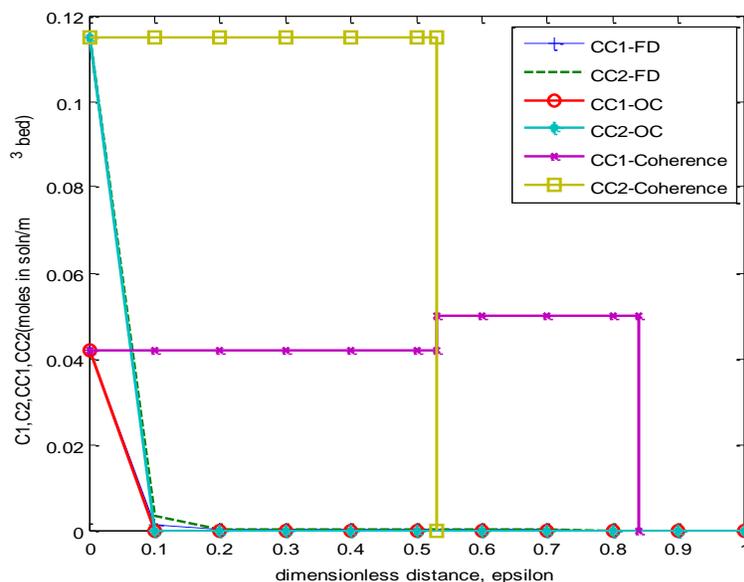
Figure 2b. Case 2. C1,C2,CC1,CC2 vs epsilon at $\tau = 2.0$. Bed composition profile for one-dimensional two-phase chromatography; Case 2, at two pore volumes injected. The plots are for three methods: Orthogonal collocation(OC), finite difference(FD) and coherent theory(CT).

There are two regions of moderate change corresponding to two "fronts". These are the leading edge of the surfactant and the solubilization (or miscible) front as the concentrations jump to their injected values. Physically, this region corresponds to the very rapid increase in the relative permeability of the aqueous phase due to the decrease in interfacial tension. This is, of course, what the surfactant is designed to do, and is a physically desirable feature of the process.

4. DISCUSSION OF RESULTS
The ultimate objective of the simulator design is the prediction of the appropriate surfactant concentration necessary for the required enhanced oil recovery from reservoirs.

The basic physical principle employed in the simulator design is the conservation of mass. Usually those quantities are conserved at stock tank conditions and related to reservoir fluid quantities through the pressure dependent parameters. The profiles for cases 1, 2 and 3 (Table 5) with one dimensional aqueous phase chromatography and two-phase chromatography for one, one-half, and two pore volume injected were developed using simulated solutions of the model equations. These equations were then solved by finite difference (FD), orthogonal collocation (OC) and coherent theory (CT).The use of these methods permits the determination of the relative efficiency of the methods and how well they predict the complex characteristics of the enhanced oil recovery process. We will now discuss the significant results of this work. We did find out that:

(i)   By injecting a mixture of an aqueous composition into a porous medium, initially devoid of surfactant, the expected composition is a self sharpening shock wave. The steepness in all the profiles generated by finite difference (FD), orthogonal collocation (OC), and coherent theory (CT) confirms the self sharpening behaviour. It may be noted in all cases that the nature the waves trajectories gradually fall, as a result of a gradual increase in the associated eigenvalues of the waves as salinity increases. The finite difference (FD) and orthogonal collocation (OC) response essentially agrees with the coherent method except except for a slight curvature. This is because the finite difference (FD) and orthogonal collocation (OC) are no longer a good approximation to the shock The consequence of this steepening is that the flows are sharpening, so that they break through both earlier and over a smaller injected volume. For the dependent variables such as

component concentration, common velocity exists at each point in the wave, and the associated composition route and relative shifts of waves associated with other dependent variable waves remains unchanged. This was confirmed for all numerical methods, in agreement with the work of Helferich[4].

(ii)   By injecting a mixture of low concentration aqueous surfactant composition into adsorbing porous medium that is initially injected with high concentration of aqueous surfactant composition, a variation may exist in the initial profile or a new profile may be generated by the injection. The initial fluid or previously injected fluid has the same composition downstream of the change while the newly injected fluid has the same composition upstream of the original variation. The composition route along the bed follows the slow path from the injected composition and then switches to the fast path leading to the previously injected compòsition. The route passes along the paths in the sequence of increasing wave velocities.

(iii)   By injecting a mixture of high concentration of surfactant into adsorbing porous medium that is initially injected with low concentration of aqueous surfactant composition, we encountered two types of path: the slow and fast paths. The slow path eigenvalues are closer to the fast path eigenvalues with values of 1; the effect of dispersion results in the merging of the two waves. This is due to their spatial position, and loss of intermediate region of constant state. However, this region later reappears as dispersion decreases.

(iv)   For a system of two phase (aqueous and oleic) flow of water and oil in which there is no surfactant partitions into the oleic phase, the effect of two phase flow is the elongation of the wave, leading to a larger region of constant state and earlier breakthrough of fast wave. The shock and wave composition routes are identical to that of the aqueous phase and has a unique composition path grid which is independent of the saturation of the flowing phases. This is similar to system of two-phase (aqueous and oleic) flow in which two water soluble components partition between an aqueous and a solid adsorbent with the use of low concentration surfactants to improve volumetric sweep efficiency during surfactant assisted waterflooding in certain enhanced oil recovery techniques[19].

(v)   When surfactant partitions into the oleic phase, the effect is that the adsorption of the surfactant in the solid phase results in the formation of micelles which then break away from the solid phase and move much faster than the surfactant in the oleic phase. The domination of the micelle formation in the aqueous phase is the general effect for both slow and fast phases. The presence of the two partitioning components does not alter the fractional flow relations $f_j(S_j)$ for the two phases.The sum of the aqueous and oleic phase saturations must add up to one wave of the saturation variables.

(vi)   The comparison between the coherent theory (CT) and finite difference (FD) and orthogonal collocation (OC) simulated results are not based on closed solutions of the transport equations, but on inexact solutions of these equations. This is in spite of the fact that the methods are based on the conservation of mass, containing the same physical properties. The slight differences are due to assumed discrete values used base on the method. The coherent wave fronts match the wave fronts for finite difference and orthogonal collocation at their points of turning, where the effective wave dispersion is zero.

The simulation results of the predicted profiles by the coherent theory (CT), finite difference (FD) and orthogonal collocation (OC) techniques illustrate the typical effects of a pattern flood such as the early breakthrough of the oil bank and the long tail on the oil surfactant curves. The results show only significant deviations in some sections. The only significant difference beween the coherent theory (CT) and finite difference (FD) results is that the finite difference (FD) profiles are continous while the coherent profiles are discontinous. More oscillations are evident in the orthogonal collocation (OC) solution profiles. This indicates that orthogonal collocation (OC) solution is sensitive to oscillation than other methods. This is particularly noticeable in the curves following breakthrough. The finite difference (FD) is considerably more dissipative and therefore the small oscillations are absent. Also the coherent suppresses oscillation and is less dissipative. These findings

are beyond the findings of Hankins and Harwell[19]. For the findings of Hankins and Harwell[19] did not show and explain these salient findings.

(vii) Several simulations were made to evaluate the dependence of oil recovery on slug size for a given amount of injected surfactant. This is an important design factor. It is generally thought that a large dilute slug will be better in a heterogeneous reservoir. This seems intuitively correct since a small slug would seem to be proportioned into the lowest permeabilities in such a small amount that little, if any, oil recovery from those parts of the reservoir could be expected. This by itself, would not be an unreasonable strategy. The dependence of oil recovery on slug size for a given amount of injected surfactant or for a fixed product of slug size and surfactant concentration indicates that the more surfactant injected, the more oil is recovered. This is because an injected surfactant disperses into oil and water, then lower the interfacial tension thereby mobilized more immobile oil. This is continued until the surfactant is diluted or lost due to adsorption by the rock. For significant incremental oil recoveries, several orders of magnitude reduction is needed. Hence, large quantities of surfactant are required for reduction of the interfacial tension to produce the desired effect. So, the effect of surfactant slug size is predictable.Also, the effect of surfactant concentration is also predictable in the same manner as more oil is recovered for increase in surfactant concentration injected.

Some of the complexities outlined above could not have been predicted by using only the coherent technique by Hankins and Harwell[24]. This is a major accomplishment of this work. Not only was the discontinuities predicted by this work, it also provides an insight into the complex behaviour of enhanced oil recovery process.

5. CONCLUSIONS

The applicability of solutions of the model transport equations for the design of the simulator in a multiphase, multicomponent flow and transport in a reservoir has been demonstrated using orthogonal collocation solution. The results of the orthogonal collocation solution were compared with those of finite difference and coherence solutions. The results obtained using this methodology revealed certain features unobserved by the published work of Hankins and Harwell[26]. The results indicate that the concentration of surfactants (C_1, C_2) for orthogonal collocation appear to show more features than the predictions of the coherence and finite difference solutions. The reason for the difference is the subject of continuing study by our team. It is unlikely that the coherence approach could ultimately accommodate the complexities required for a thorough understanding of the full field reservoir simulator.

It is obvious that the coherent routes for the compositions of adsorbing surfactants correspond to the simpler case of aqueous phase chromatography, with modified eigenvalue. This observation also holds for "shock" waves. The existence of a partially coherent solution makes the prediction of reservoir response much more straightforward. However, the 'partially' coherent solution only exist if surfactants does not partition into the oleic phase and fractional flow is not a function of surfactant composition; should either occur, a globally coherent solution may still be found, but the solution is more complex and difficult to handle. There is no equivalence of partial coherence in the orthogonal and finite difference methods. Therein lies the possibility of the differences in the concentration profiles predicted by the three numerical techniques. Again, the use of the orthogonal collocation and finite difference solution provides easier solution to future possible problems that may arise as the simulator is being used.

The dependence of oil recovery on slug size for a given amount of injected surfactant indicates that the more surfactant injected the more oil is recovered. For significant incremental oil recoveries, several order of magnitude interfacial tension reduction is needed. Hence, large quantities of surfactant are required to produce the desired effect of high oil recovery.

TABLE 1

Reservoir characteristics from the work of Hankins and Harwell[24]

Parameter	Value
Rock density	2.65 g/cm^3
Porosity	0.2
Oil viscosity	5.0 cp
Water viscosity	1.0 cp
Injection pressure gradient (maintained constant)	1.5 psi/ft
Fluid densities	1.0 g/cm^3
Width of injection face	50 ft
Width of central high permeability streak	10 ft
Length of reservoir	100 or 5000 ft
Residual oil saturation	0.2
Connate water saturation	0.1
First injected surfactant	SDS
Second injected surfactant	DPC
Henry's law constant SDS DPC	2.71×10^{-4} l/g 8.30×10^{-5} l/g
CMC Values SDS DPC	800 μmol/l 4000 μmoll/l
Injected concentration SDS DPC	10 CMC 10 CMC
Brine spacer (typical)	≈ 0.05 pore volumes
Slug volumes	≈ 0.10 pore volumes

TABLE 2

Reservoir Characteristics used for the Simulation work by Oyedeko [25]

Parameter	Value
Rock density	2.65 g/cm^3
Porosity	0.2
Oil viscosity	0.40 cp
Water viscosity	0.30 cp
Injection pressure gradient (maintained constant)	1.5 psi/ft
Fluid densities	1.0 g/cm^3
Width of injection face	50 ft
Width of central high permeability streak	10 ft
Length of reservoir	100 or 5000 ft
Residual oil saturation	0.2
Connate water saturation	0.2
First injected surfactant	SDS
Second injected surfactant	DPC
Henry's law constant SDS DPC	2.71×10^{-4} l/g 8.30×10^{-5} l/g
CMC Values SDS DPC	800 μmol/l 4000 μmoll/l
Injected concentration SDS DPC	10 CMC 10 CMC
Brine spacer (typical)	≈ 0.05 pore volumes
Slug volumes	≈ 0.10 pore volumes

TABLE 3

Parameter values used in Trogus adsorption model for verification runs[26]

Parameter	Value
Pure component CMCs	$C_1^* = 1.0$ mol/m^3 $C_2^* = 0.35$ mol/m^3
Phase separation model parameter	$\theta = 1.8$
Henry's law constants for adsorption	$\bar{C_i} = k_i C_{i,w}$ ($C_{i,w}$ = aqueous monomer concentration) $k_1 = 0.21 \times 10^{-3}$ m^3/kg $k_2 = 0.80 \times 10^{-3}$ m^3/kg
Henry's law constant for oleic partitioning	$C_{i,o} = q_i C_{i,w}$ ($C_{i,w}$ = aqueous monomer concentration) $q_1 = 7.1$ $q_2 = 1.3$
Adsorbent properties	$\rho_s = 2.1 \times 10^{+3}$ m^3/kg $\emptyset = 0.2$

TABLE 4

Additional Reservoir Parameters for the coherence work by Hankin and Harwell (2004)[24]

Model designation	A	B
Grid points in the horizontal direction (m+1)	21	21
Grid points in the vertical direction (n+1)	11	21
Coherent waves of water saturation	28	28

Initial number of points per coherent wave
     Water
     Surfactant
	
	 41
	 81
		
		 41
		 81

Maximum number of points required per coherent wave	≈ 300	≈ 300

Average time step size (days)
   Short reservoir (100 ft)
     200 mD streak
     1000 mD streak
   Long reservoir (5000ft)
     200 mD streak
     1000 mD sreak
	
	 3.47
	 0.69
	
	 174.0
	 34.7
		
		 3.47
		 0.69
		
		 174.0
		 34.7

Typical number of time steps required to inject first pore volume
  Short reservoir
  Long reservoir
	
	 33
	 75
		
		 33
		 75

TABLE 5

Conditions for case studies of surfactant chromatography by Hankin and Harwell (2004)[24]

Case	Injected composition: $CC1(mol/m^3 bed)$	Injected composition: $CC2(mol/m^3 bed)$	Initial composition: $C1(mol/m^3 bed)$	Initial composition: $C2(mol/m^3 bed)$
1	0.17	0.013	0.21	0.181
2	0.042	0.115	0	0
3	0.66	0.875	0.35	0.15

6. REFERENCES

[1]. J. Glimm, B. Lindquist, O.A. McBryan, B. Plohr, B. and S. Yaniv. Front Tracking for Petroleum Reservoir Simulation. Paper SPE 12238 Presented at the seventh SPE Symposium on Reservoir Simulation, San Francisco, Nov. 16-18, 1983. Society of Petroleum Engineers of AIME, Dallas, Texas (USA).

[2]. R,E.Ewing, T.F. Russel and M.F. Wheeler. Simulation of Miscible Displacement using Mixed Methods and a Modified Method of Characteristics. Paper SPE 12241 Presented at the seventh SPE Symposium on Reservoir Simulation, San Francisco, Nov. 16-18, 1983. Society of Petroleum Engineers of AIME, Dallas, Texas (USA).

[3]. C. Zheng. Extension of the Method of Characteristics for Simulation of Solute Transport in 3 Dimensions. Ground Water, 1993, 31(3): 456-465.

[4]. F.G. Helfferich. Theory of Multicomponent, Multiphase Displacement in Porous Media. Soc. Pet. Eng. J., 1981, 21: 51-62.

[5]. L.W. Lake. Enhanced Oil Recovery. London: Prentice-Hall, 1989.

[6]. E.F. Dezabala, J.M. Vislocky, E. Rubin and C.J. Radke. A Chemical Theory for Linear Alkaline Flooding. Soc. Pet. Eng. J., 1982, 22: 245-258.

[7]. G.I. Hirasaki. Application of the Theory of Multicomponent, Multiphase Displacement to Three-Component, Two-Phase Surfactant Flooding. Soc. Pet. Eng. J., 1981, 21: 191-204.

[8]. L.W. Lake. and F.G. Helfferich. Cation Exchange in Chemical Flooding: Part 2. The effect of dispersion, cation exchange, and polymer/surfactant adsorption on chemical flood environment. Soc. Pet. Eng. J., 1978, 18: 435-444.

[9]. F.G. Helfferich. The Theory of Precipitation/Dissolution Waves. AIChE J., 1989, 35(1): 75-87.

[10]. A. Araque-Martinez, and L.W. Lake. Some Frequently Overlooked Aspects of Reactive Flow through Permeable Media. Ind. Eng. Chem. Res., 2000, 39(8): 2717-2724.

[11].N.P. Hankins and F.G. Helfferich. On the Concept and Application of Partial Coherence in Non-linear Wave Propagation. Chem. Eng. Sci. 1999, 54: 741-764.

[12]. H.M. Helset and L.W. Lake. Three-phase Secondary Migration of Hydrocarbon. Math. Geol., 1998, 30(6): 637-660.

[13]. O.A. Cirpka, and P.K. Kitanidis.Transport of Volatile Compounds in Porous Media in the Presence of a Trapped Gas Phase. J. Contam. Hydrol., 2001, 49(3-4): 263-285.

[14]. J.R. Patton, K.H. Coats and G.T. Colegrove. Prediction of Polymer Flood Performance. Soc.Pet. Eng., 1971, 11: 72-84.

[15]. F.J. Fayers and R.I. Perrine. Mathematical Description of Detergent Flooding in Oil Reservoirs. Petroleum Trans. AIME, 1959, 216: 277-283.

[16]. E.L. Claridge and P.I. Bondor. (1974). A Graphical Method for Calculating Linear Displacement with Mass Transfer and Continuously Changing Mobilities. Soc. Pet. Eng. J., 1974, 14; 609-618.

[17]. R.G. Larson. The Influence of Phase Behaviour on Surfactant Flooding. Soc. Pet. Eng. J., 1979, 19: 411-422.

[18]. G.A. Pope, G.F. Carey and K. Sepehrnoori. Isothermal, Multiphase, Multicomponent Fluid Flow in Permeable Media. Part II: Numerical Techniques and Solution. In Situ, 1984, 8(1): 1-40

[19] N.P. Hankins and J.H. Harwell. Case Studies for the Feasibility of Sweep Improvement in Surfactant-assisted Waterflooding. J. Pet. Sci. Eng., 1997, 17: 41-62.

[20]. L. Siggel, M. Santa, M. Hansch, M. Nowak, M. Ranft, H. Weiss, D. Hajnal, E. Schreiner, G. Oetter, G. and J. Tinsley. A New Class of Viscoelastic Surfactants for Enhanced Oil Recovery BASFSE SPE Improved Oil Recovery Symposium, 14-18 April, 2001, Tulsa, Oklahoma, USA

[21]. Y. Xu, and M. Lu. Microbially Enhanced Oil Recovery at Simulated Reservoir Conditions by Use of Engineered Bacteria. J. Petr. Sci. Eng., 2001, 78(2): 233-238.

[22]. A. Leach, A. and C.F. Mason. Co-optimization of Enhanced Oil Recovery and Carbon Sequestration. J. Resource and Energy Economics. Resourse Energy Econ., 2011, 33(4): 893-912.

[23]. J.H. Harwell. Enhanced Oil Recovery Made Simple. J. Petr. Technol., 2012, 60(10): 42-43.

[24] N.P. Hankins. and J.H. Harwell. Application of Coherence Theory to a Reservoir Enhanced Oil Recovery Simulator. J. Pet. Sci. Eng., 2004, 42: 29-55.

[25]. K.F. Oyedeko. Design and Development of a Simulator for a Reservoir Enhanced Oil Recovery Process. PhD Dissertation, Lagos State University, Ojo, Lagos, Nigeria, 2014.

[26]. F.J. Trogus, R.S. Schecchter, G.A. Pope and W.H. Wade. New Interpretation of Adsorption Maxima and Minima. J. Colloid Interface Sci., 1979, 70(3): 293-305.

[27]. F.G. Helfferich. Multicomponent Wave Propagation: Attainment of coherence from arbitrary starting conditions. Chem. Eng. Comm., 1986, 44: 275-285.

[28] J.V. Villadsen and W.E. Stewart. Solution of Boundary Value Problems by Orthogonal Collocation. Chem. Eng. Sci., 1967, 22: 1483-1501.

[29] J.V. Villadsen and W.E. Stewart. Solution of Boundary Value Problems by Orthogonal Collocation. Chem. Eng. Sci., 1968, 23: 1515.